



**Fermi National Accelerator Laboratory**

FERMILAB-Conf-74/55-E

Inclusive  $\gamma K^0(s)$   $\Lambda^0$  and Anti- $\Lambda^0$  Production  
in  $205\text{GeV}/c \pi^- p$  Interactions

Dixon Bogert et al.

*Fermi National Accelerator Laboratory*

*P.O. Box 500, Batavia, Illinois 60510*

1974

## INTRODUCTION

This paper presents preliminary results of a study of inclusive  $\gamma$ ,  $K_S^0$ ,  $\Lambda^0$  and  $\bar{\Lambda}^0$  production in 205 GeV/c  $\pi^-p$  interactions. The experimental data were in 48,000 frames from the FERMILAB 30-inch bubble chamber filled with hydrogen. Results on inclusive neutral cross sections using approximately one-half the film have been previously reported.<sup>1</sup>

## EVENT SELECTION AND WEIGHTING

A total of 1644 gamma conversions or neutral decays were associated with the 7000  $\pi^-p$  events found in the film.<sup>2</sup> These gamma conversions or neutral decays were classified on the scan table as 273 G's (Gammas, defined as having at least one identified electron), 520 V's (Vees, defined as having a non-zero opening angle), and 851 A's (Ambiguous, defined as zero opening angle and no identified electrons). This breakup into G, V, or A at the scan table was useful for the preliminary analysis of events,<sup>3</sup> and it was necessary for an understanding of the scanning efficiency for gamma conversions and neutral decays (see below). During measurement and editing 3.6% of these GVA's were rejected as being incorrectly picked up by the scanners (for example, 1.9% did not point to the associated event). Another 31% were discarded by a fiducial volume cut.<sup>4</sup> The remaining 1068 in the fiducial volume were processed through TVGP and SQUAW. Seven percent of these

events failed to reconstruct in TVGP even after two or more measurements. In SQUAW kinematic fits to  $\gamma(p) \rightarrow e^- e^+ p$ ,  $K_S^0 \rightarrow \pi^- \pi^+$ ,  $\Lambda^0 \rightarrow \pi^- p$ , and  $\bar{\Lambda}^0 \rightarrow \bar{p} \pi^+$  were attempted.<sup>5</sup> For each fit a chi-squared and the transverse momentum of the positive ( $p_t^+$ ) and negative ( $p_t^-$ ) outgoing tracks relative to the neutral track were calculated. Acceptable fits were defined as having a chi-squared less than 20 and both  $p_t$  less than 15 MeV/c for  $\gamma$  fits or  $p_t^-$  greater than 15 MeV/c for neutral decay fits. The  $p_t$  cut was introduced to help resolve ambiguities between gamma conversions and neutral decays. After these cuts there were 119 events with no acceptable fit, 815 events with one unique fit, and 61 ambiguous events with two acceptable fits. There were 41  $K_S^0$   $\Lambda^0$  ambiguities, 19  $K_S^0$   $\bar{\Lambda}^0$  ambiguities, and one  $\gamma$   $\bar{\Lambda}^0$  ambiguity, and they were resolved by choosing the fit with the lowest chi-squared. The final sample contained 485  $\gamma$  fits, 248  $K_S^0$ 's, 118  $\Lambda^0$ 's, and 25  $\bar{\Lambda}^0$ 's. From a study of the decay angle in the center of mass of the neutral particle it was estimated that the final sample of  $K_S^0$ 's has 4% contamination from  $\Lambda^0$  and  $\bar{\Lambda}^0$  decays, and that the  $\Lambda^0$  and  $\bar{\Lambda}^0$  samples have 8% and 16%  $K_S^0$  contamination respectively.

In order to determine the total number of gamma conversions and neutral decays produced at the primary vertex, each event with a fit was weighted by the product of five separate weights. The first weight was the inverse of the conversion<sup>6</sup> or decay probability as determined by the particle's momentum and potential length inside the fiducial

volume. Secondly, each neutral decay was weighted by the inverse of the branching ratio for the particular decay mode observed. The events failing to reconstruct in TVGP or failing to fit in SQUAW were studied, and it was found that most of these events were enmeshed in the tracks from the primary vertex and that the failures were due to measurement difficulties. It was also found that certain classes of conversions and decays had a higher percentage of unmeasurable events than others and hence all events were classified according to whether they were scanned as a G, a V, or an A and according to the charged prong multiplicity of the associated primary vertex. Then the events with fits in each classification were weighted appropriately to account for the unmeasurable events. The fourth weight was applied to V's and A's found close to the primary vertex, to correct for those missed in the scan (all G's were found due to their distinct electron spiral tracks). Finally, it was discovered that the scanning efficiency for A's was lower than that for G's and V's. Even after a double scan nine percent of the A's were missed, and so all events scanned as A's were weighted to correct for this scanning inefficiency. The average weights were: 89.6 for  $\gamma$ , 3.59 for  $K_S^0$ , 3.56 for  $\Lambda^0$ , and 5.83 for  $\bar{\Lambda}^0$ . The difference in the  $\Lambda^0$  and  $\bar{\Lambda}^0$  weights is due to the difference in the  $\Lambda^0$  and  $\bar{\Lambda}^0$  momentum distributions (see  $F_1(x)$  distributions below).  $K_S^0$ 's,  $\Lambda^0$ 's, and  $\bar{\Lambda}^0$ 's produced forward in the center of mass generally escape this chamber before decaying. Thus, there are only a small number of detected fast forward neutrals

in the final sample, and they have large weights. They are kept as they are the only source of information on forward produced neutrals, but one must remember that the statistics are very poor in the forward hemisphere.

### CROSS SECTION RESULTS

Tables I-IV give the number of fitted events, inclusive cross sections as a function of  $n_{ch}$  (the number of charged particles produced), and the average number of neutrals produced per inelastic collision, for  $\gamma$ 's,  $K_S^0$ 's,  $\Lambda^0$ 's, and  $\bar{\Lambda}^0$ 's respectively. Forward and backward cross sections are given for neutrals with  $x$  greater than zero and less than zero respectively ( $x \equiv \frac{2p_L}{\sqrt{s}}$ ,  $p_L$  and  $s$  calculated in center of mass). In Table I,  $\langle n_{\pi^0} \rangle$  is calculated assuming all  $\gamma$ 's come from the decay  $\pi^0 \rightarrow \gamma\gamma$ . Figure 1 compares the neutral inclusive cross sections in this experiment with lower energy data for  $\pi^\pm p$  interactions.<sup>7,8,9</sup> The  $\pi^0$ ,  $K_S^0$  and  $\Lambda^0$  cross sections have approximately doubled from 20 GeV/c while the  $\bar{\Lambda}^0$  cross section has increased one order of magnitude. Figures 2-5 show the average number of neutral particles produced per inelastic interaction as a function of the number of charged particles produced. In Fig. 2 note that the number of  $\pi^0$ 's produced rises linearly with the number of charged particles (mostly pions) produced (at least up through  $n_{ch} = 14$ ). For 10.5 GeV/c  $\pi^+ p$  interactions,<sup>7</sup>  $\langle n_{\pi^0} \rangle$  is flat as a function of  $n_{ch}$ , while for 25 GeV/c  $\pi^- p$  interactions,<sup>9</sup> one sees the start of a linear dependence of  $\langle n_{\pi^0} \rangle$

on  $n_{ch}$ . Thus, the correlation between neutral and charged pion production appears to become stronger as the beam momentum increases. In contrast to neutral pion production, the production of  $K_S^0$ 's,  $\Lambda^0$ 's, and  $\bar{\Lambda}^0$ 's, Figs. 3-5, appears to have little or no correlation with charged particle production. The backward neutral particle decay results can be compared with 205 GeV/c pp results. If it is assumed one can "factorize" an interaction into a forward part associated with the beam particle and a backward part associated with the target, then the results on particles produced backward per inelastic interaction for  $\pi^-p$  at a given momentum should be approximately the same as comparable results for pp interactions at the same momentum. Table V shows that the results of this experiment agree very well with the corresponding results for 205 GeV/c pp.<sup>10</sup>

### MOMENTUM DEPENDENCE

The dependence of neutral particle production on the longitudinal momentum of the produced particle is shown in Figs. 6-9 for  $\gamma$ ,  $K_S^0$ ,  $\Lambda^0$  and  $\bar{\Lambda}^0$  production respectively. Here,  $F_1(x)$  is the invariant double differential cross section integrated over  $p_T^2$ ,

$$F_1(x) \equiv \frac{2}{\pi \sqrt{s}} \int_0^{\infty} \frac{E d^2\tau}{dx dp_T^2} dp_T^2,$$

where all quantities are calculated in the center of mass. First, note that these distributions depend strongly on the produced particle. In particular,  $\Lambda^0$  production is peaked in the backward direction, indicating production by target fragmentation. Figure 6 may indicate that forward  $\gamma$  production is somewhat different from backward  $\gamma$  production. Figure 7 shows that  $K_S^0$  production occurs in the central region with a possible plateau for  $|x| < 0.1$ .

Figures 10-13 show  $F_2(p_T^2)$  distributions for the four produced particles.  $F_2(p_T^2)$  is the invariant double differential cross section integrated over  $x$ ,

$$F_2(p_T^2) \equiv \frac{2}{\pi \sqrt{s}} \int_{-1}^{+1} \frac{E d^2\sigma}{dx dp_T^2} dx .$$

Note that the steepness of the exponential falloff is a function of the mass of the produced neutral. That is, the  $F_2$  distribution falls fastest  $\gamma$ 's and is flattest for  $\Lambda^0$  production.

REFERENCES

- \* Work supported in part by the U. S. Atomic Energy Commission, the National Science Foundation, and the French CNRS.
- † Present address: LAL, Orsay, France.
- ‡ On leave from the Université de Paris VI, Paris, France.
- § Present address: Department of Physics, California Institute of Technology.
- \*\* Guggenheim Fellow, on sabbatical leave at CERN.
- <sup>1</sup> D. Bogert et al., "Inclusive  $\gamma$ ,  $K_S^0$ ,  $\Lambda^0$  and  $\bar{\Lambda}^0$  Production by 205 GeV/c  $\pi^-p$  Interactions" (submitted to Berkeley Meeting of the American Physical Society, 1973), and D. Ljung, "Experimental Inclusive  $\gamma$ ,  $K_S^0$ ,  $\Lambda$  and  $\bar{\Lambda}$  Production," AIP Conference Proceedings - Berkeley, 1973, p. 464.
- <sup>2</sup> Analysis of 3114 of these events and further experimental details are given in D. Bogert et al., Phys. Rev. Letters 31, 1271 (1973).
- <sup>3</sup> For example, the correction to charged particle cross sections due to close gamma conversions and close neutral decays that were missed on the scan table was helped by this classification, as it was found that essentially only A's were missed.
- <sup>4</sup> The neutral vertex was required to be inside a cylinder of radius 25 cm and height 23 cm centered in the bubble chamber. The primary vertex was required to be in a fiducial volume of length 33.4 cm in the beam

direction with an entrance plane 12 cm downstream of the bubble chamber window.

<sup>5</sup>Kaon decay results refer only to  $K_S^0$  as  $K_L^0$  particles generally leave this chamber before decaying. Also, this experiment cannot tell the difference between lambda's produced directly and lambda's produced from the decay of  $\Sigma^0$ . Thus  $\Lambda^0$  refers to  $\Lambda^0$  or  $\Sigma^0$  production and  $\bar{\Lambda}^0$  refers to  $\bar{\Lambda}^0$  or  $\bar{\Sigma}^0$  production.

<sup>6</sup>For gamma conversion the pair production cross sections given in T. M. Knasel, DESY Reports Nos. 70/2 and 70/3, 1970 (unpublished) were used.

<sup>7</sup>M. E. Binkley et al., Phys. Letters 45B, 295 (1973). (10.5 GeV/c  $\pi^+$  p interactions.)

<sup>8</sup>P. H. Stuntebeck et al., Phys. Rev. D9, 608 (1973). (18.5 GeV/c  $\pi^-$  p interactions.)

<sup>9</sup>Jerome William Elbert, "High Multiplicity Pion Production in 25 GeV/c Pi-Minus-Proton Collisions," University of Wisconsin thesis, 1971. (Note that events with strange particle production were excluded from this cross section.)

<sup>10</sup>K. Jaeger et al., "Production of Strange Particles and of  $\gamma$ -Rays in Proton-Proton Interactions at 205 GeV/c," ANL paper submitted to Berkeley Meeting of the American Physical Society, August 13-17, 1973.

Their  $\Lambda^0$  and  $\bar{\Lambda}^0$  results have been divided by two in order to get a result for the backward hemisphere (making use of forward-backward symmetry in pp experiments). The  $K^0$  result has been divided by four because they included  $K_L^0$  in their calculation.

TABLE I

Cross Sections for  $\pi^- p \rightarrow \gamma + \text{Anything}$ 

Number of Charged Particles Produced $n_{ch}$	Number of Fitted $\gamma$ 's	$\sigma_{n_{ch}}(\gamma)$ mb	$\langle n_{\pi^0} \rangle$ per inelastic interaction
2	13	$5.4 \pm 1.6$	$1.7 \pm 0.5$
4	47	$17.9 \pm 3.4$	$2.5 \pm 0.5$
6	76	$33.1 \pm 5.5$	$4.2 \pm 0.7$
8	86	$30.1 \pm 4.3$	$3.6 \pm 0.5$
10	98	$32.2 \pm 4.4$	$4.8 \pm 0.7$
12	83	$27.0 \pm 4.2$	$6.1 \pm 1.0$
14	40	$12.7 \pm 2.5$	$5.7 \pm 1.1$
16	18	$4.7 \pm 1.3$	$3.8 \pm 1.0$
18	17	$5.5 \pm 1.9$	$8.9 \pm 3.0$
20	6	$1.8 \pm 0.8$	$9.0 \pm 3.8$
22	1	$0.12 \begin{matrix} + 0.60 \\ - 0.06 \end{matrix}$	$2.3 \begin{matrix} + 11.6 \\ - 1.2 \end{matrix}$
Total	485	$170.6 \pm 15.3$	$4.06 \pm 0.36$
Forward	272	$87.4 \pm 8.9$	--
Backward	213	$83.2 \pm 9.1$	--

TABLE II

Cross Sections for  $\pi^- p \rightarrow K_S^0 + \text{Anything}$ 

Number of Charged Particles Produced $n_{ch}$	Number of Fitted $K_S^0$	$\sigma_{n_{ch}}(K_S^0)$ mb	$\langle n_{K_S^0} \rangle$ per inelastic interaction
0	1	$0.008 \pm 0.041$ $- 0.004$	$0.82 \pm 4.10$ $- 0.41$
2	8	$0.51 \pm 0.45$	$0.31 \pm 0.27$
4	35	$0.56 \pm 0.14$	$0.16 \pm 0.04$
6	48	$0.56 \pm 0.11$	$0.14 \pm 0.03$
8	39	$0.46 \pm 0.11$	$0.11 \pm 0.03$
10	56	$0.59 \pm 0.11$	$0.18 \pm 0.03$
12	33	$0.45 \pm 0.10$	$0.21 \pm 0.05$
14	10	$0.11 \pm 0.04$	$0.09 \pm 0.04$
16	11	$0.14 \pm 0.05$	$0.23 \pm 0.08$
18	7	$0.11 \pm 0.05$	$0.35 \pm 0.17$
Total	248	$3.49 \pm 0.60$	$0.166 \pm 0.029$
Forward	54	$1.64 \pm 0.50$	$0.078 \pm 0.024$
Backward	194	$1.85 \pm 0.23$	$0.088 \pm 0.011$

TABLE III

Cross Sections for  $\pi^- p \rightarrow \Lambda^0 + \text{Anything}$ 

Number of Charged Particles Produced $n_{ch}$	Number of Fitted $\Lambda^0$	$\sigma_{n_{ch}} (\Lambda^0)$ mb	$\langle n_{\Lambda^0} \rangle$ per inelastic interaction
2	16	$0.34 \pm 0.16$	$0.204 \pm 0.098$
4	22	$0.21 \pm 0.06$	$0.060 \pm 0.016$
6	22	$0.24 \pm 0.07$	$0.060 \pm 0.018$
8	23	$0.31 \pm 0.11$	$0.076 \pm 0.027$
10	21	$0.30 \pm 0.09$	$0.091 \pm 0.026$
12	9	$0.20 \pm 0.09$	$0.088 \pm 0.039$
14	3	$0.05 \pm 0.03$	$0.042 \pm 0.027$
16	1	$0.005^{+0.026}_{-0.003}$	$0.008^{+0.041}_{-0.004}$
18	1	$0.004^{+0.022}_{-0.002}$	$0.014^{+0.069}_{-0.007}$
Total	118	$1.65 \pm 0.33$	$0.079 \pm 0.016$
Forward	7	$0.46 \pm 0.20$	$0.022 \pm 0.010$
Backward	111	$1.19 \pm 0.21$	$0.057 \pm 0.010$

TABLE IV

Cross Sections for  $\pi^- p \rightarrow \bar{\Lambda}^0 + \text{Anything}$ 

Number of Charged Particles Produced $n_{\text{ch}}$	Number of Fitted $\bar{\Lambda}^0$	$\sigma_{n_{\text{ch}}}(\bar{\Lambda}^0)$ mb	$\langle n_{\bar{\Lambda}^0} \rangle$ per inelastic interaction
2	1	$0.06^{+0.06}$ $-0.04$	$0.038^{+0.038}$ $-0.025$
4	3	$0.06 \pm 0.04$	$0.017 \pm 0.011$
6	8	$0.15 \pm 0.08$	$0.038 \pm 0.020$
8	5	$0.10 \pm 0.06$	$0.023 \pm 0.015$
10	4	$0.11 \pm 0.07$	$0.033 \pm 0.019$
12	3	$0.06 \pm 0.05$	$0.029 \pm 0.020$
14	0	--	--
16	1	$0.03^{+0.06}$ $-0.02$	$0.048^{+0.097}$ $-0.028$
Total	25	$0.57 \pm 0.22$	$0.027 \pm 0.010$
Forward	6	$0.25 \pm 0.13$	$0.012 \pm 0.006$
Backward	19	$0.32 \pm 0.13$	$0.015 \pm 0.006$

TABLE V

Comparison of Backward Neutral Particles Produced Per  
Inelastic Interaction for 205 GeV/c  $\pi^-$ p and pp

Neutral Particle	$\langle n \rangle_{\pi^- p}$	$\langle n \rangle_{pp}^a$
$K_S^0$ (backward)	$0.088 \pm 0.011$	$0.085 \pm 0.005$
$\Lambda^0$ (backward)	$0.057 \pm 0.010$	$0.055 \pm 0.005$
$\bar{\Lambda}^0$ (backward)	$0.015 \pm 0.006$	$0.013 \pm 0.004$

<sup>a</sup>Reference 10.

## FIGURE CAPTIONS

- Fig. 1 Neutral inclusive cross sections as a function of beam momentum for  $\pi^{\pm}p$  interactions.
- Fig. 2 Average number of  $\pi^0$ 's produced per inelastic interaction as a function of the number of charged particles produced.
- Fig. 3 Average number of  $K_S^0$ 's produced per inelastic interaction as a function of the number of charged particles produced.
- Fig. 4 Average number of  $\Lambda^0$ 's produced per inelastic interaction as a function of the number of charged particles produced.
- Fig. 5 Average number of  $\bar{\Lambda}^0$ 's produced per inelastic interaction as a function of the number of charged particles produced.
- Fig. 6  $F_1(x)$  as a function of  $x$  for  $\gamma$  production.
- Fig. 7  $F_1(x)$  as a function of  $x$  for  $K_S^0$  production.
- Fig. 8  $F_1(x)$  as a function of  $x$  for  $\Lambda^0$  production.
- Fig. 9  $F_1(x)$  as a function of  $x$  for  $\bar{\Lambda}^0$  production.
- Fig. 10  $F_2(p_T^2)$  as a function of  $p_T^2$  for  $\gamma$  production.
- Fig. 11  $F_2(p_T^2)$  as a function of  $p_T^2$  for  $K_S^0$  production.
- Fig. 12  $F_2(p_T^2)$  as a function of  $p_T^2$  for  $\Lambda^0$  production.
- Fig. 13  $F_2(p_T^2)$  as a function of  $p_T^2$  for  $\bar{\Lambda}^0$  production.

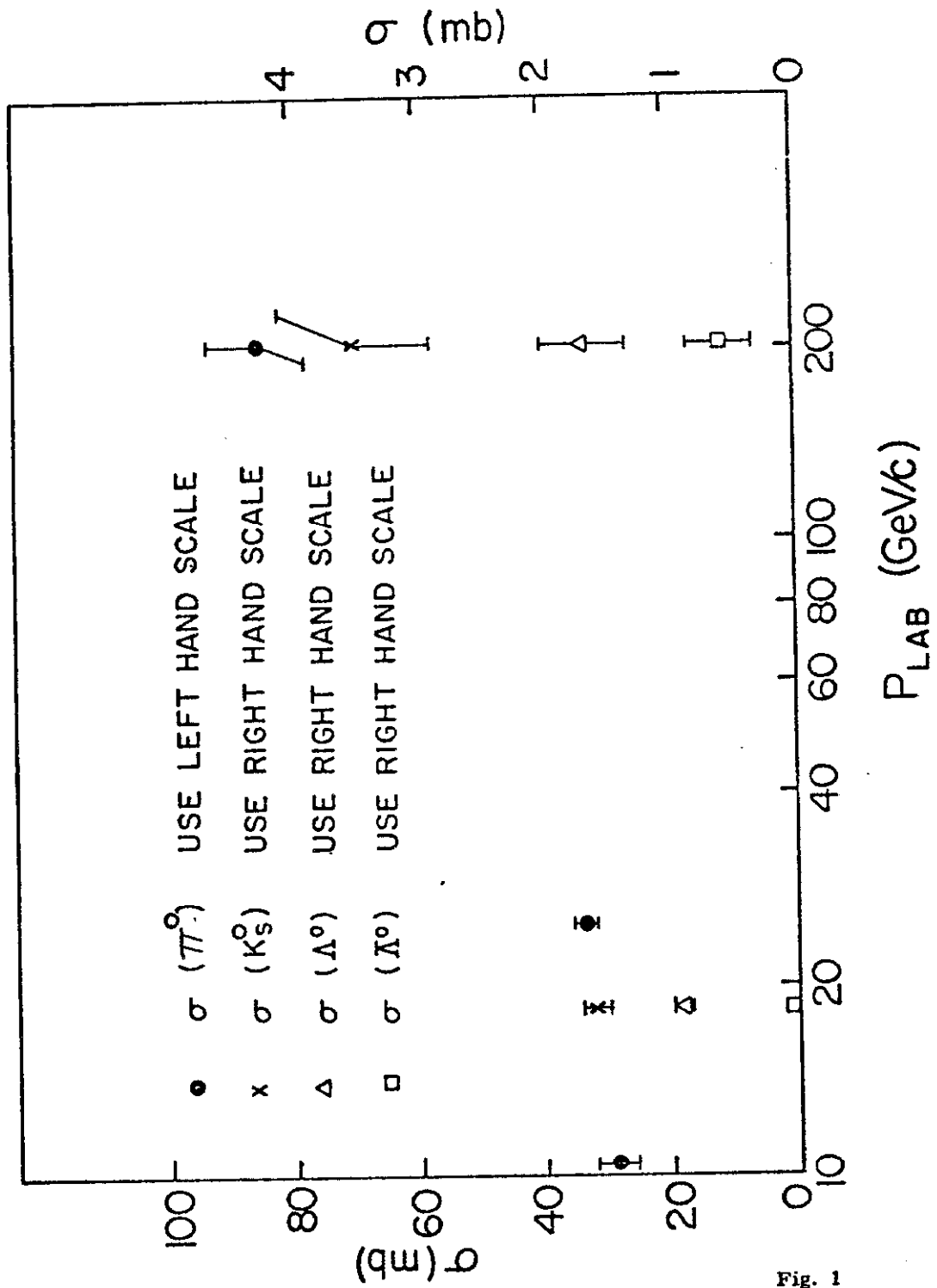


Fig. 1

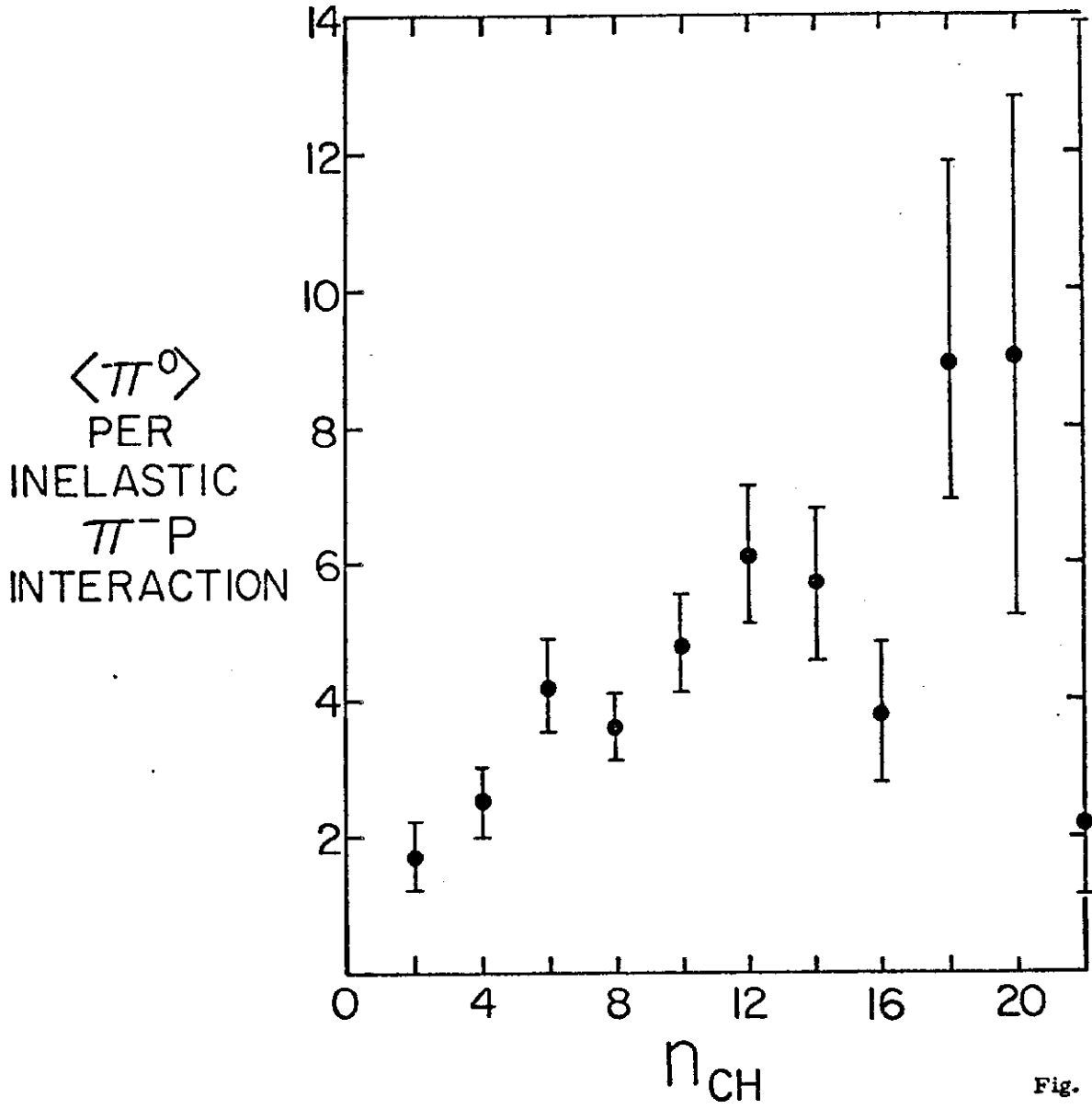


Fig. 2

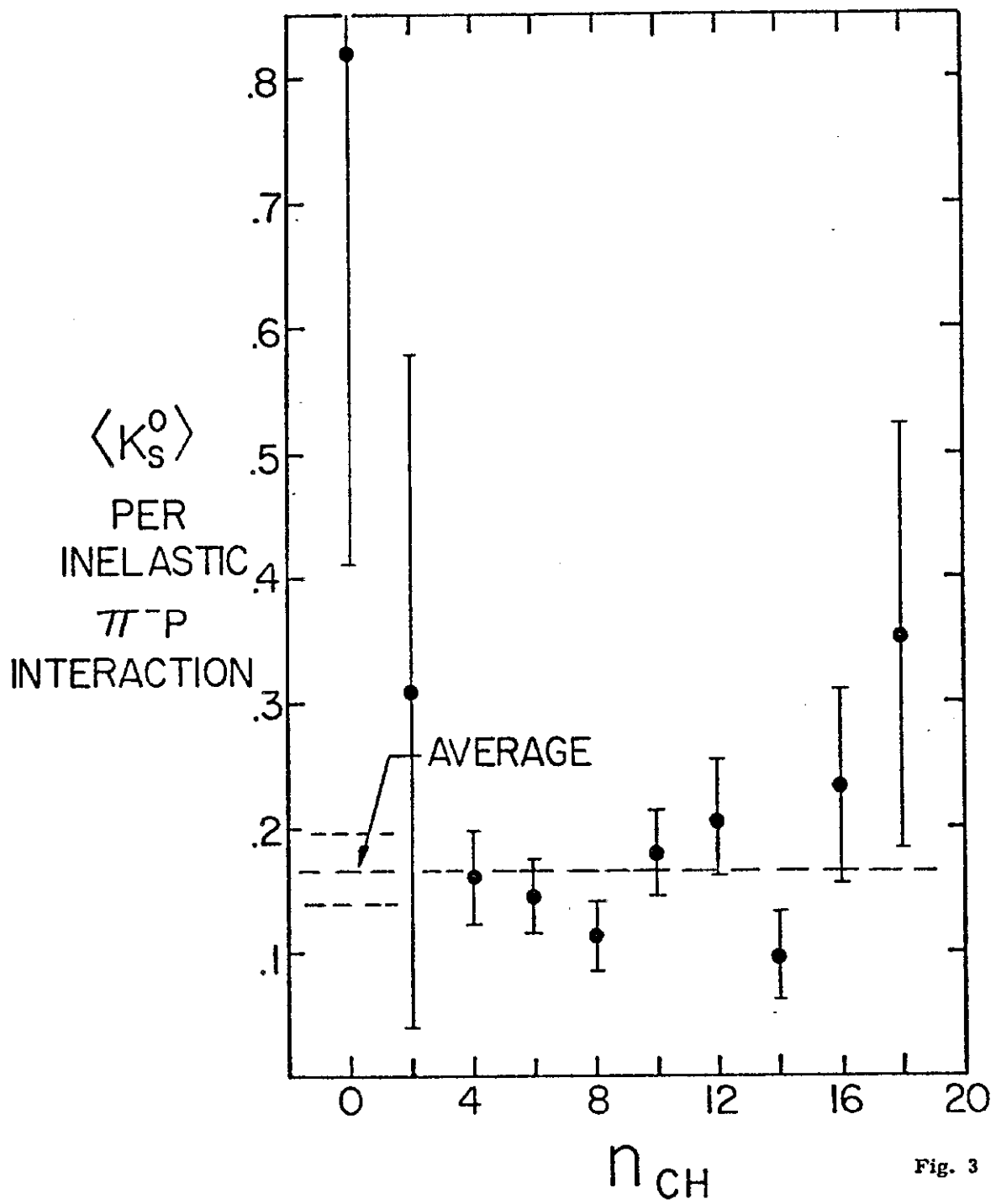


Fig. 3

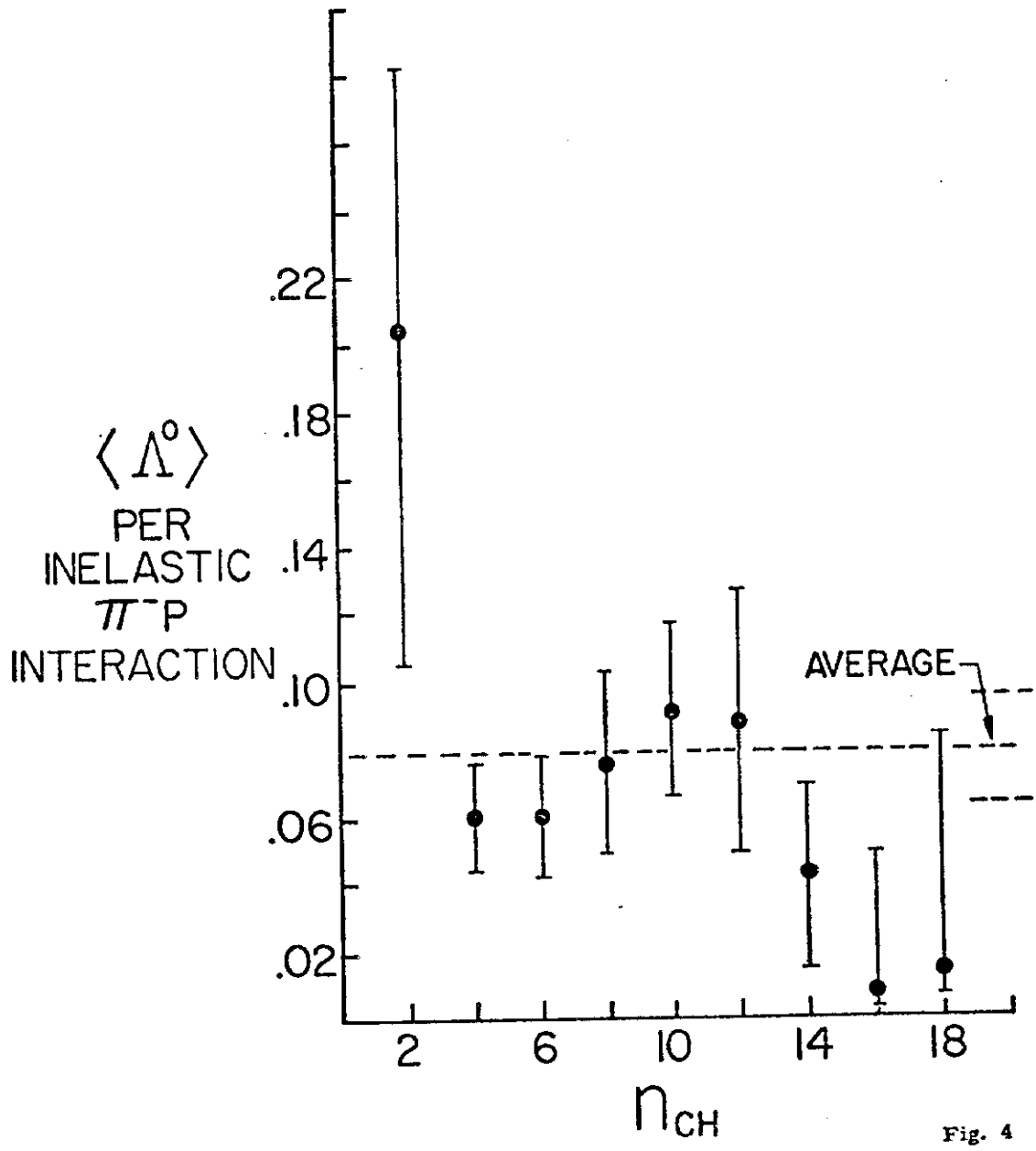


Fig. 4

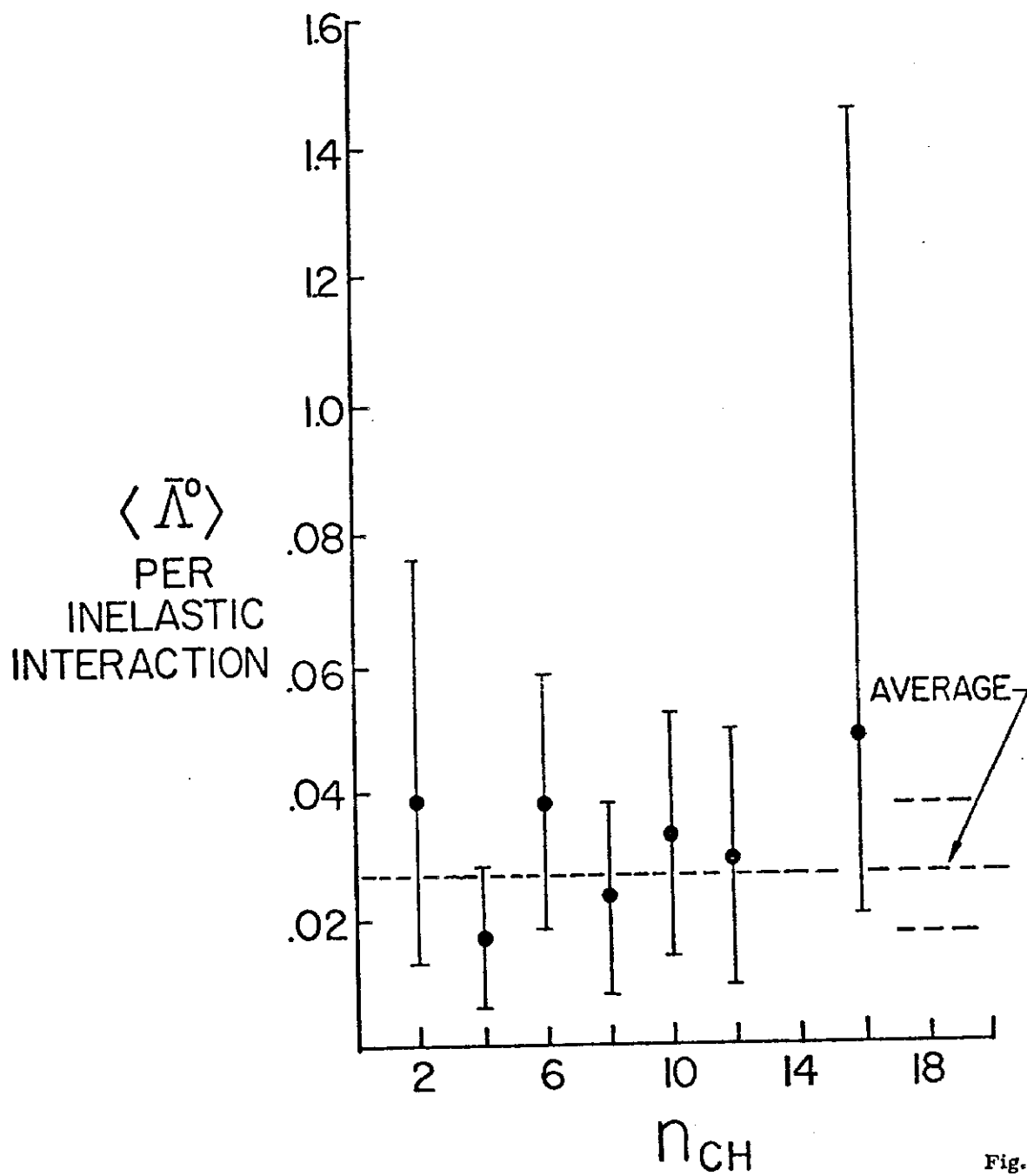


Fig. 5

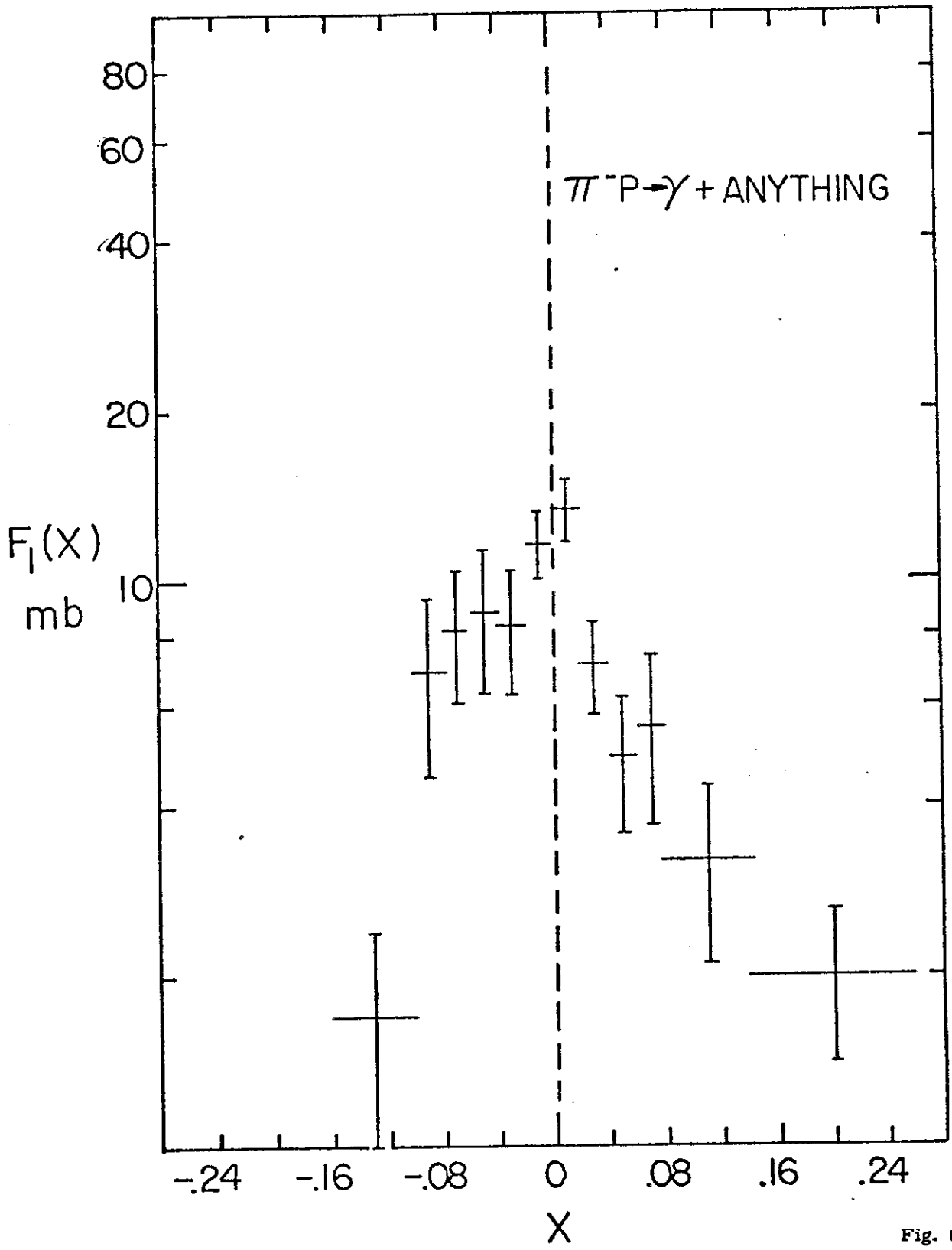


Fig. 6

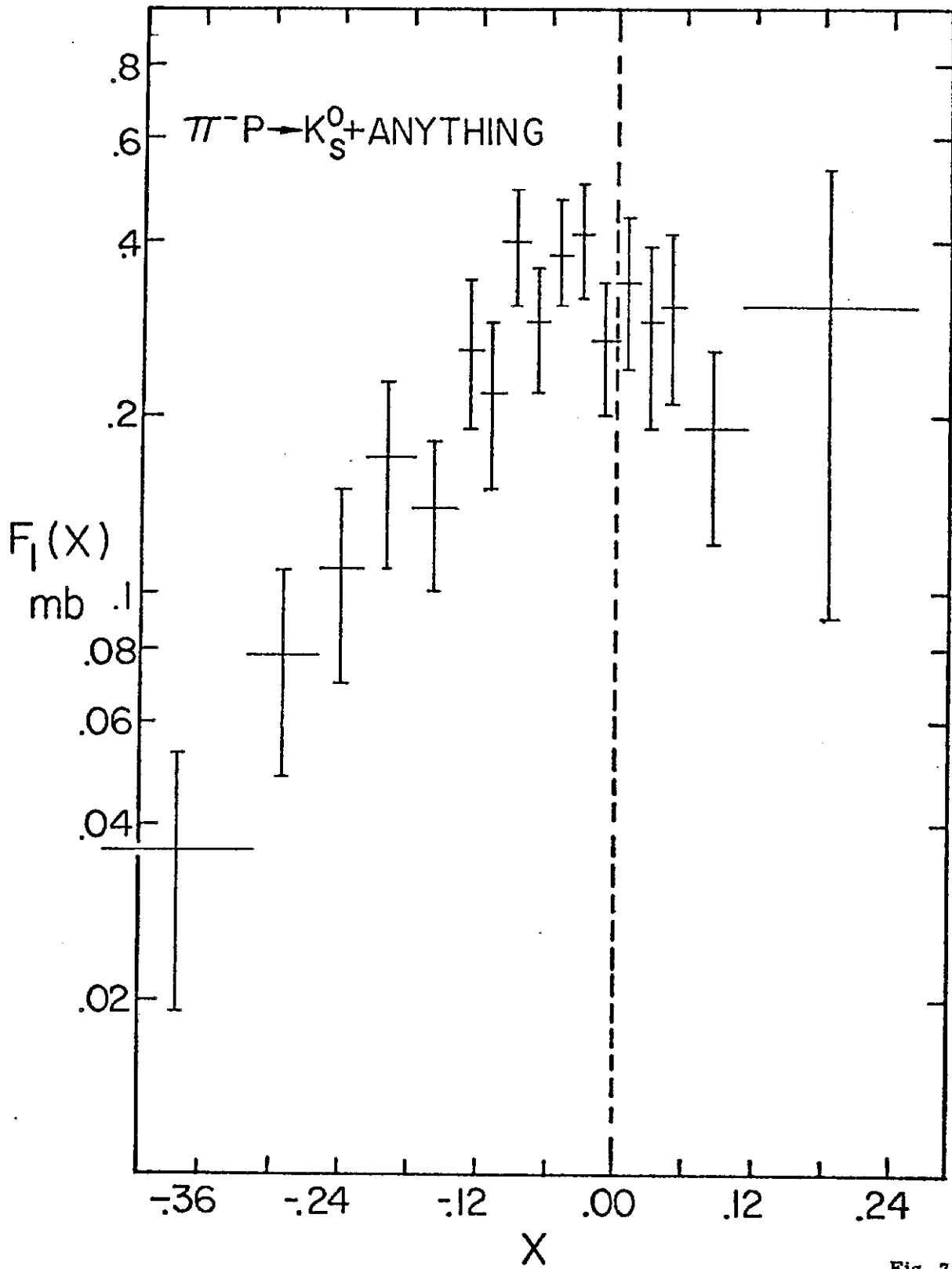


Fig. 7

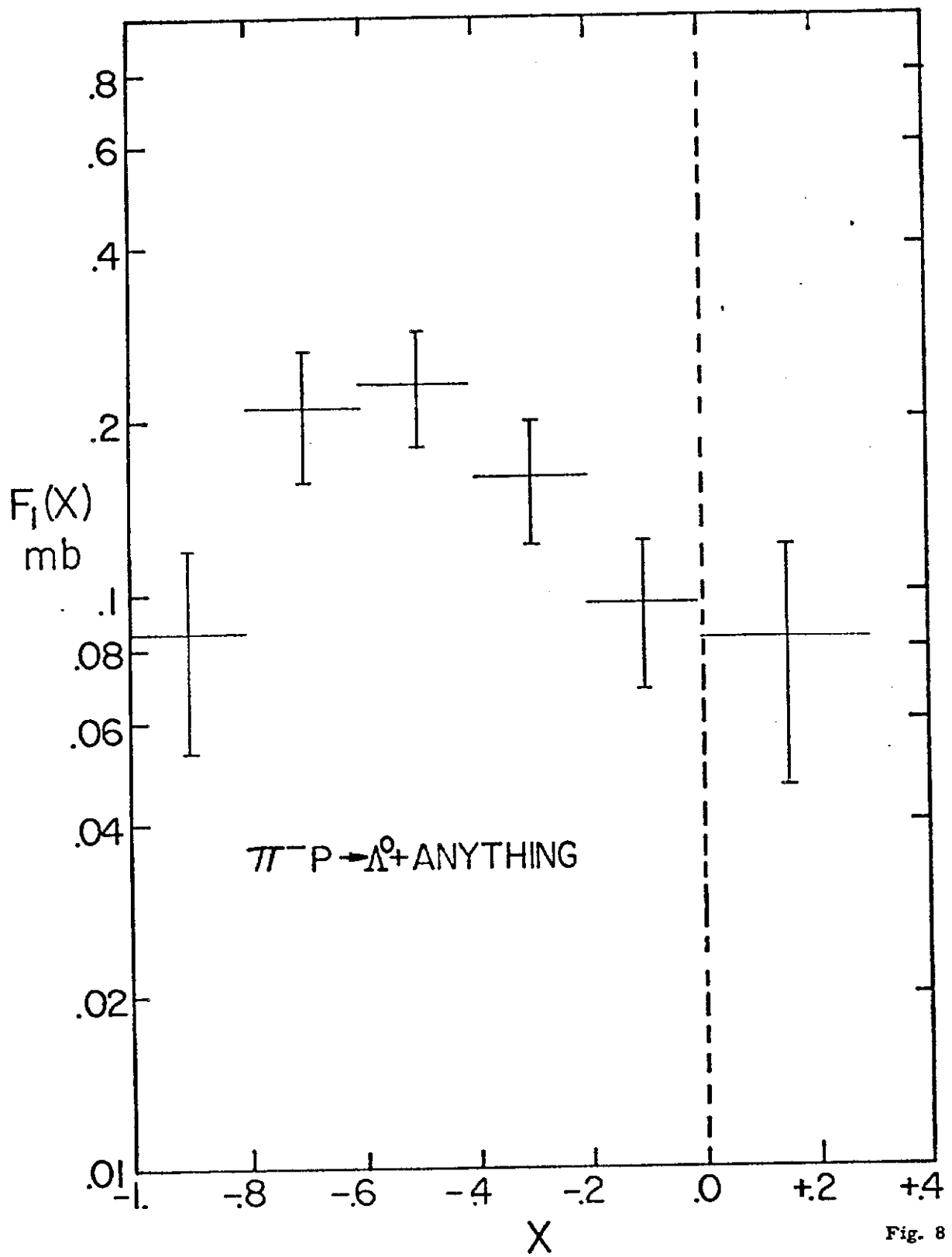


Fig. 8

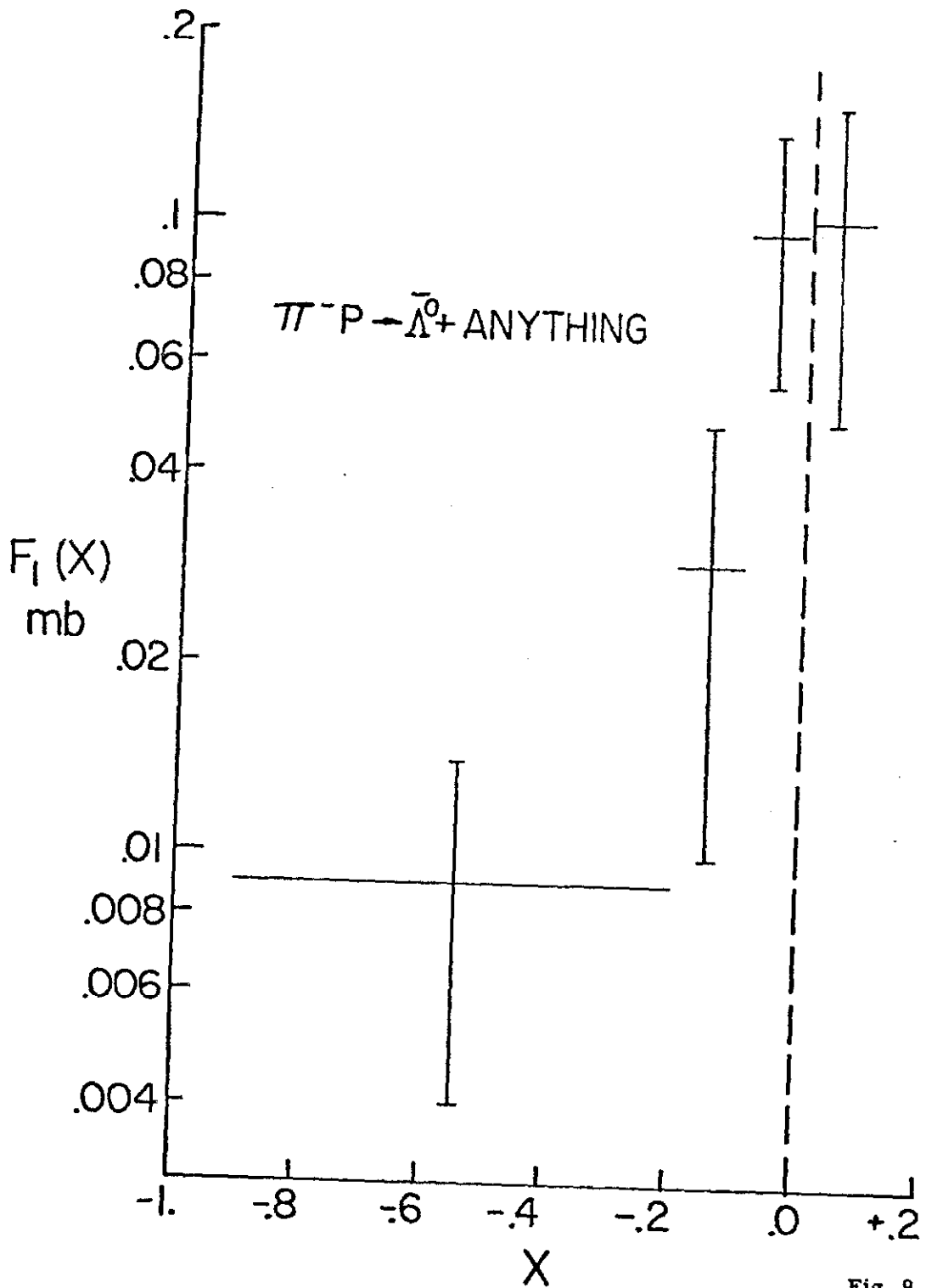


Fig. 9

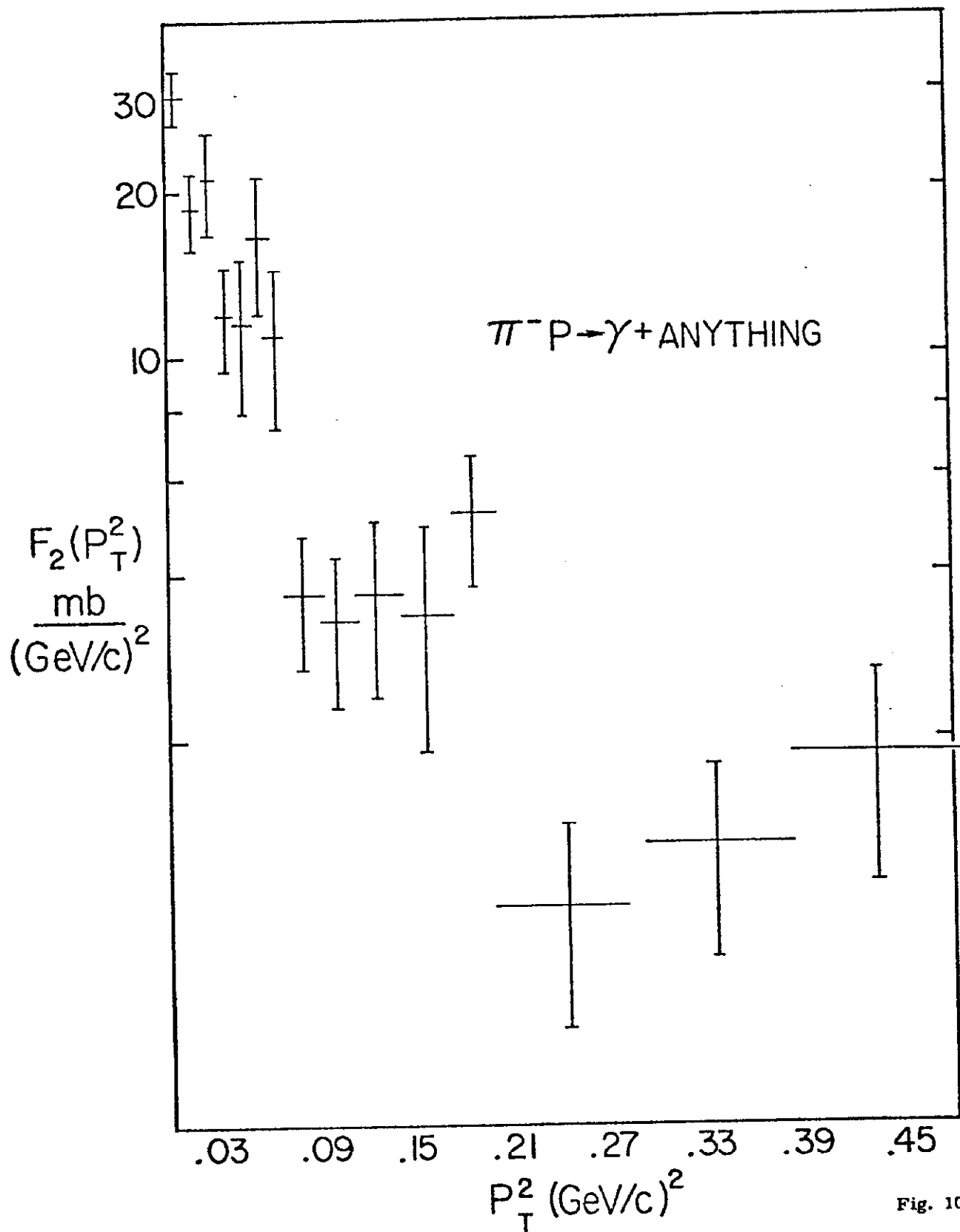


Fig. 10

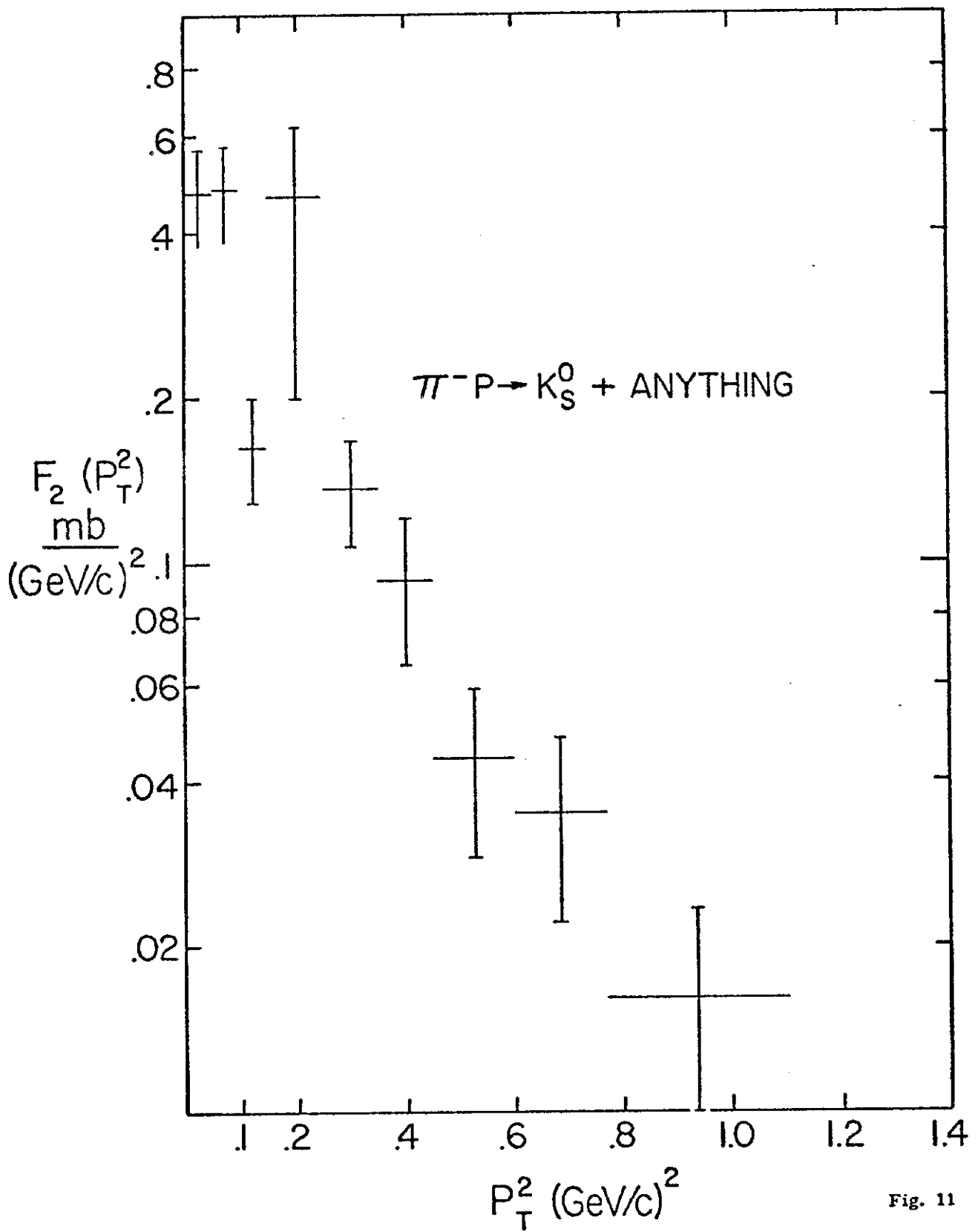


Fig. 11

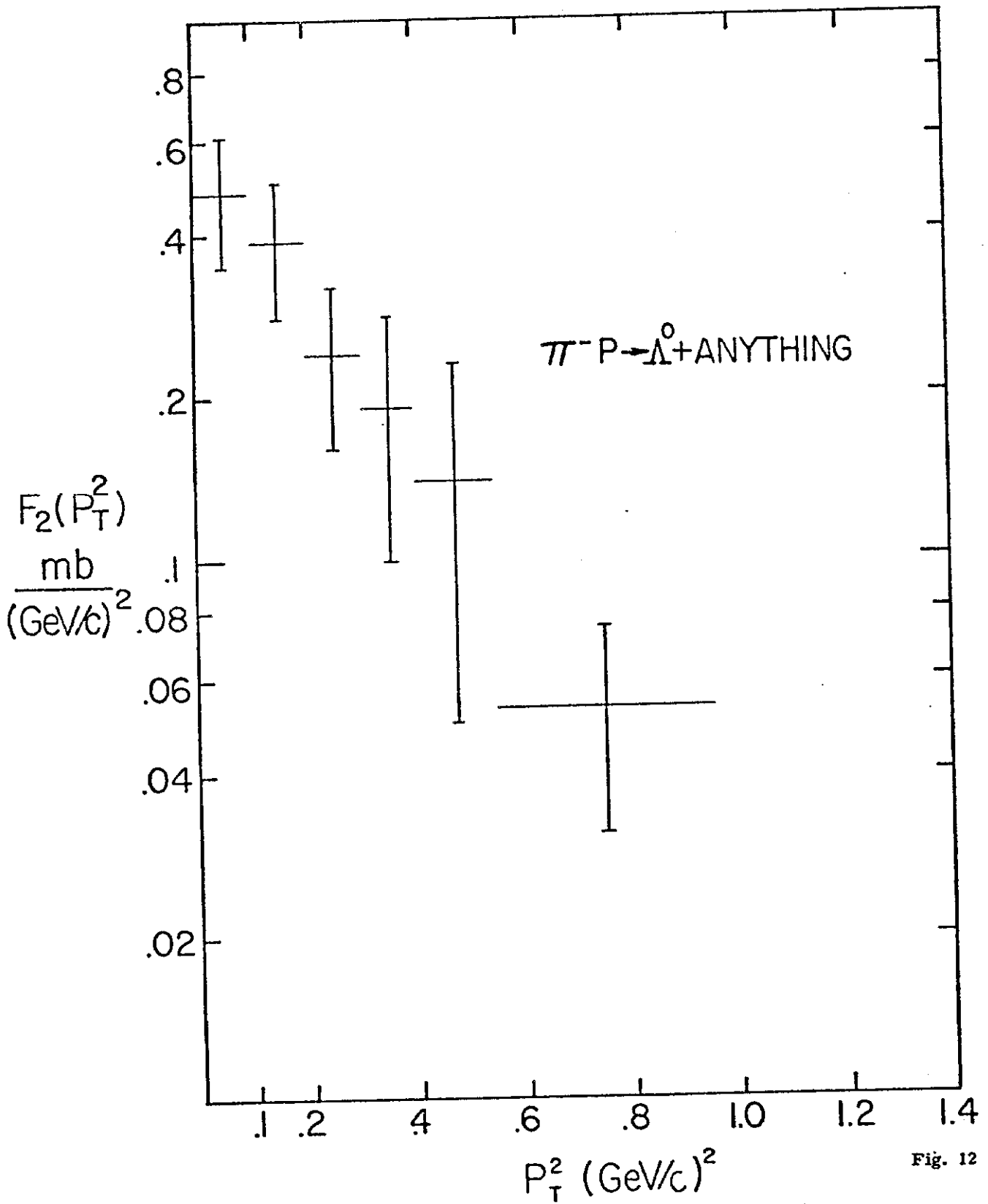


Fig. 12

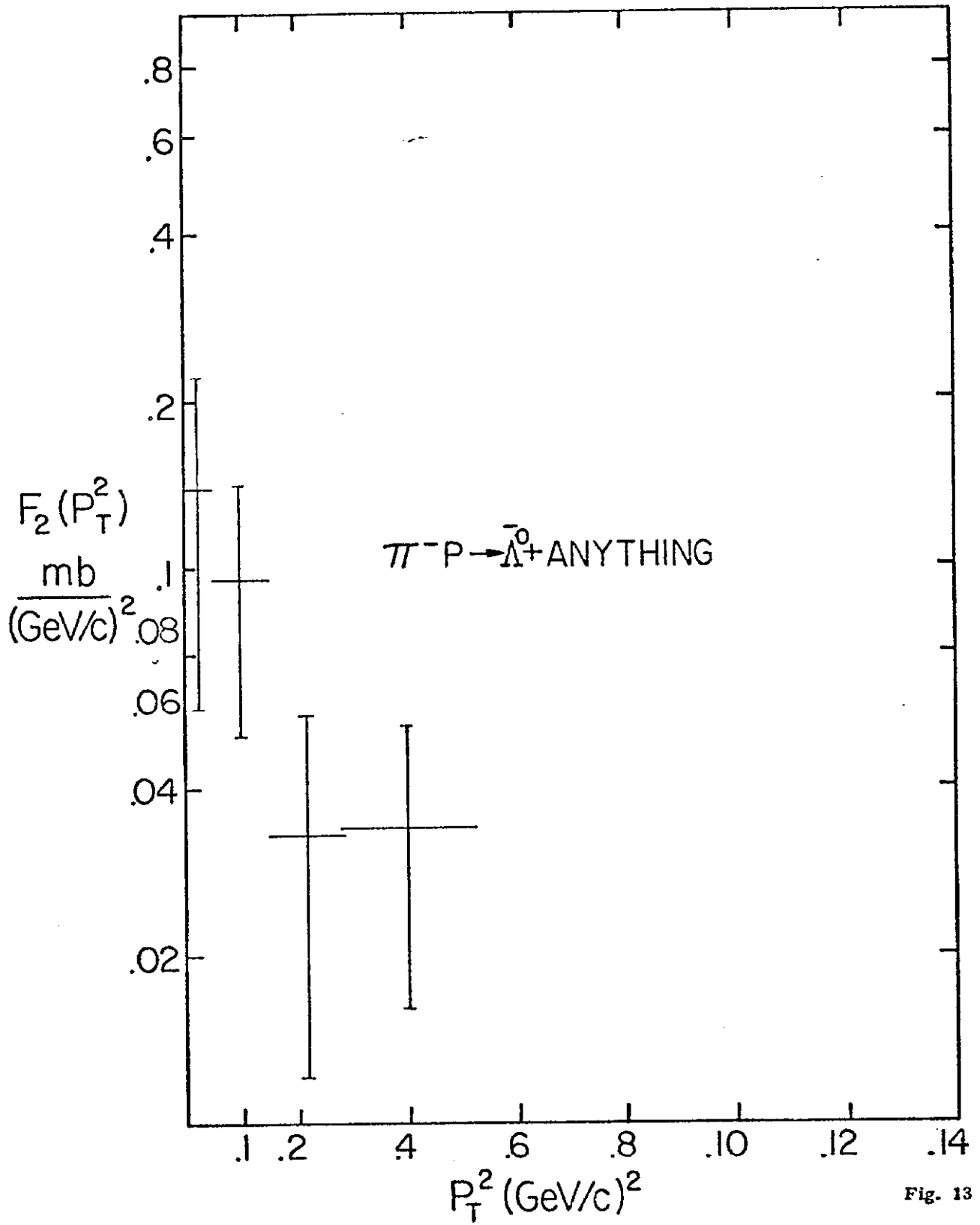


Fig. 13